POSITRON CAMERA WITH EXTENDED COUNTING RATE CAPABILITY

Gerd Muehllehner

Searle Analytic Inc., Searle Radiographics Inc., Des Plaines, Illinois

Positron emitters may be imaged using two opposing scintillation cameras without collimators. The counting rate limitation of this approach can be largely overcome by using graded absorbers to reduce scattered radiation from the patient and using not only photopeak events but Compton events in the scintillator as well. This increases the useful counting rate by more than a factor of 5. By combining this technique with the use of fast electronics, useful images have been obtained in the presence of scattering material at counting rates above 7,500 cps.

TABLE 1. INTERACTIONS IN SODIUM IODIDE*

Probability of interaction	½-in. NaI at 510 keV	½-in. NaI at 150 keV
Any kind	0.349	0.939
Compton first	0.293	0.232
Photoelectric first	0.056	0.707
Compton first followed by escape of secondary photon	0.179	0.030
One or more Compton followed by a photoelectric interaction	0.114	0.202
Photopeak interaction	0.169	0.909

* From Anger and Davis (5).

Positron imaging is a promising technique for radioisotope imaging not only because new and powerful radioisotopes can be used but also because of potential advantages in both resolution and sensitivity. It has been slow to gain widespread use because no adequate imaging device is being offered commercially and because the radioisotopes are not generally and easily available.

Among the efforts to build a positron-imaging device, the work under the direction of Brownell (*1*) is particularly noteworthy. Very high counting rate capability was stressed, but since it is a device using multiple scintillation crystals for position determination, resolution is limited by the size of the crystals and higher resolution is again achieved by sacrificing sensitivity. On the other hand, efforts have been undertaken to combine two Anger scintillation cameras in coincidence to image positrons (*2,3*). Scintillation cameras have suffered from a lack of counting rate capability but have the attractive feature that commercially available equipment can be used with a minimum of modification and additional electronics. Furthermore, high resolution can be obtained without sacrificing sensitivity.

In the present work, we have combined two Anger scintillation cameras to build a positron-imaging device and have reduced the counting rate problem significantly. Graded absorbers were used to reduce scattered radiation from the patient (*4*). This makes it possible to use Compton interactions in the scintillation crystal to form the image. Using the Compton interactions in a positron camera consisting of two Anger scintillation cameras increases the useful counting rate fivefold through better quantum utilization without any corresponding increase in the dose to the patient. Combined with fast pulse-handling electronics, this technique made it possible to achieve counting rates above 10,000 cps in laboratory experiments. We conclude from this that imaging times of less than 1 min can be expected in a clinical situation.

ENERGY SPECTRA

A gamma ray entering a scintillation crystal may either undergo a photoelectric interaction or a Compton interaction followed by either a later photoelectric interaction of the secondary gamma ray or by escape of the secondary gamma ray from the crystal. The probability of either event occurring as a function of gamma ray energy and crystal thickness has been studied by Anger and Davis (*5*). Table 1

Received Oct. 23, 1974; revision accepted Jan. 22, 1975.

For reprints contact: Gerd Muehllehner, Searle Analytic Inc., Searle Radiographics Inc., 2000 Nuclear Dr., Des Plaines, Ill. 60018.

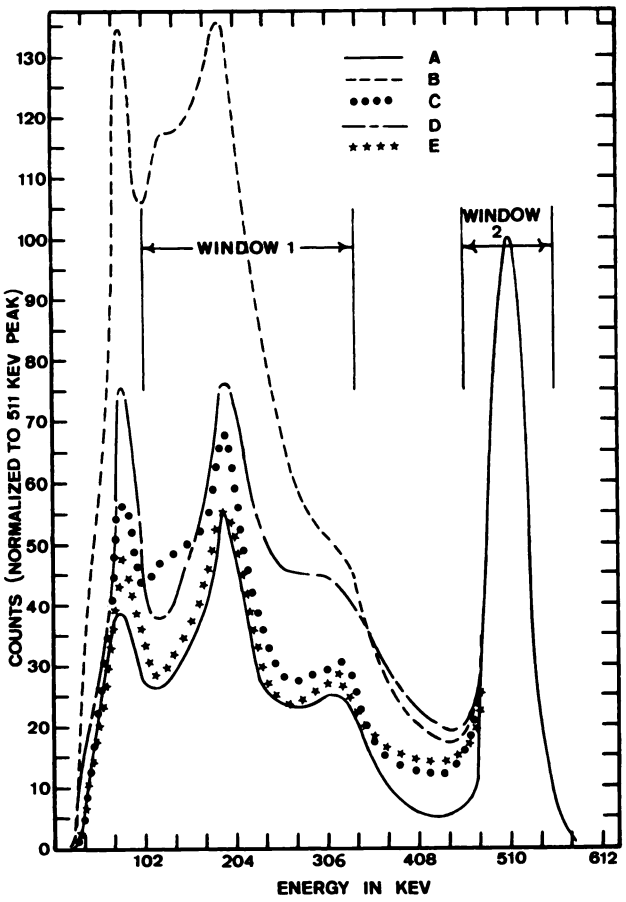

FIG. 1. Energy spectra of ^{18}F under various conditions: A, no scatter material, coincidence, or absorber; B, with scatter material, no coincidence, or absorber; C, with scatter material, coincidence, but no absorber; D, with scatter material, no coincidence, with absorber; and E, with scatter material, coincidence, and absorber.

shows the various probabilities for a ½-in.-thick NaI(Tl) crystal for gamma ray energies of 150 keV and 510 keV. A sharp contrast is immediately evident. While at 150 keV most gamma rays interact in the crystal and specifically most result in a photopeak interaction, at 510 keV a large percentage (65%) do not interact with the crystal at all. Of the 35% that do interact roughly only half result in a photopeak interaction while the other half interact through Compton scattering followed by escape of the secondary photon. A typical spectrum is shown in Fig. 1, Curve A; of course, both photopeak events as well as Compton events are potentially useful for image formation since in each case the centroid of the light emitted during the scintillation corresponds quite closely to the location at which the gamma ray entered the crystal. In the past only the photopeak interactions have been used in positron cameras consisting of opposed Anger cameras (*2,3*) since radiation scattered within the imaged object, whose point of interaction in the crystal bears no significant relation to its origin, falls into the same energy band as Compton events. Figure 1, Curve B shows the energy spectrum of a point source surrounded by scattering material, the difference between Curves A and B being due to the scattered radiation from the object. It can be seen that the majority of the counts below the photopeak are due to scattered radiation from the object.

In order to display the scatter spectrum directly, the primary radiation was largely blocked from reaching the detector using lead shielding (Fig. 2, Curve B). Contrary to the shape of the scatter spectrum for lower gamma ray energies (*6*), most scattered radiation has energies well below the energy of the primary radiation. An absorber of appropriate thickness placed between the object and the detector will attenuate the primary radiation very little but will attenuate the scattered radiation by a substantial amount. A second absorber can then be used to attenuate the characteristic x-rays from the first absorber (*4*). Figure 2 also shows the scatter spectrum with a graded absorber of 1.27 mm lead, 0.76 mm tin, and 0.25 mm copper stacked in the order listed with the lead foil facing the object. This absorber attenuates the primary radiation by only 20% while eliminating a large fraction of the scattered radiation. Thus the possibility exists of eliminating most scattered radiation from the patient with graded absorbers, transmitting most primary radiation, and then using not only photopeak events but also Compton events occurring in the crystal for image formation.

In order to test and verify experimentally whether the lower energy interactions can be used in forming an image in a positron camera without leading to an unacceptable background due to the acceptance of some scattered radiation and in order to determine

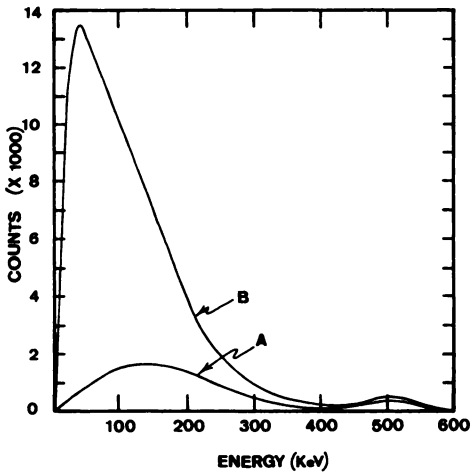

FIG. 2. Scatter spectrum for 511-keV primary radiation (most primary radiation blocked from reaching detector) with (A) and without (B) graded absorber accumulated for equal time.

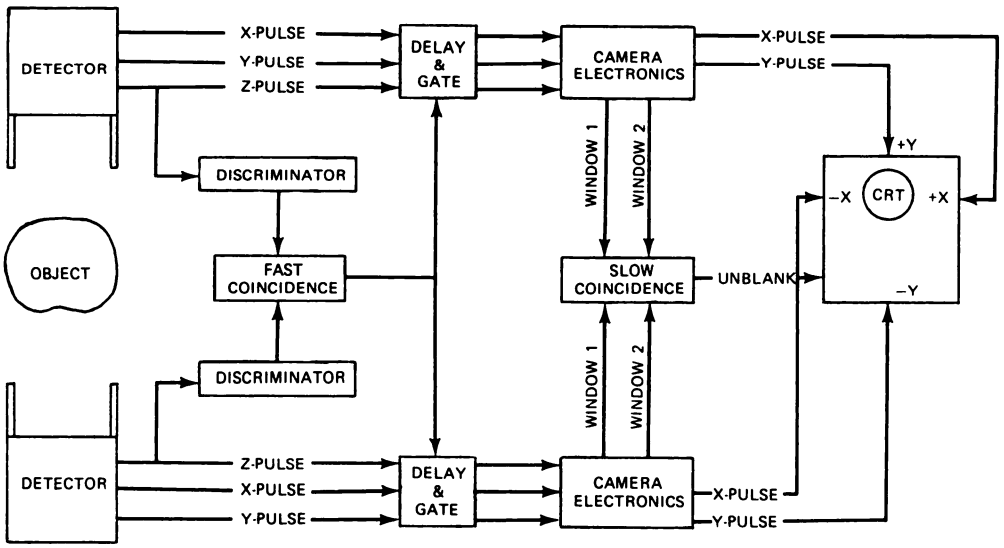

FIG. 3. Block diagram of electronics.

the resultant increase in counting rate, a positron camera was built consisting basically of two Anger scintillation cameras. A block diagram is shown in Fig. 3. Coincidence of two events is determined before most pulse processing since only roughly 10% of all pulses are coincident. Two energy windows are used in each camera, one centered on the photopeak, the other spanning the energy interval from approximately 100 keV to 340 keV. Counts falling between the two windows are predominantly forward-scattered gamma rays from the object which are only poorly discriminated against by the absorbers and which also pass the coincidence requirement. Counts falling below 100 keV are not being used for image formation since lead x-rays from shielding material fall into this energy region and since below 100 keV the spatial resolution of the camera worsens rapidly. A slow coincidence unit allows the selection of coincidences of all combinations of windows, i.e., photopeak–photopeak, photopeak–Compton, Compton–photopeak, and Compton–Compton coincident interactions.

The energy spectra A and B of Fig. 1 were obtained without requiring coincidence; they are a representation of events occurring in the detector itself. If one gamma ray is scattered through a large angle, there is only a small probability that it will reach the opposing detector and will be found in coincidence (*1*). The energy spectrum for pulses which are coincident shows therefore a sharp decrease in scattered gamma rays (Fig. 1, Curve C). Similarly, placing an absorber (1.27 mm lead) in front of both detectors also decreases scattered gamma rays even if coincidence is not required (Fig. 1, Curve D). The main difference lies in the fact that in one case the electronics is busy rejecting scattered gamma rays some appreciable fraction of the time, and in the other case the absorber prevents the scattered gamma rays from entering the detector, thereby reducing the number of scattered and mostly noncoincident events being analyzed by the coincidence electronics. Figure 1, Curve E shows that the energy spectrum with scattering material, with absorber and requiring coincidence, is similar in shape to the energy spectrum without scattering material, suggesting that the combination of absorber and coincidence requirement is indeed effective in rejecting scattered radiation from the object.

LINE-SPREAD FUNCTIONS AND PHANTOM RESULTS

Line-spread functions were measured with the line source suspended in a cylindrical volume of water 5 in. in diam and 5.5 in. high as scattering material. Line-spread functions for photopeak–photopeak coincidences (A), Compton–Compton coincidences (B), and all four possible combinations (C) are shown in Fig. 4 together with the respective counting rates. When all coincident counts in both windows are used for image formation, a system resolution of approximately 10 mm full width at half maximum (FWHM) is achieved with a background due to scattered radiation which is marginally higher than that obtained with a low-energy emitter such as ^{99m}Tc (*7*). The increase in counting rate from 260 cps (photopeak–photopeak coincidences) to 1,400 cps (all combinations) represents more than a fivefold gain. Figure 5 shows the image of a thyroid phantom surrounded by water as scatter material allowing all coincident combinations of Compton and photopeak events (same conditions as in Fig. 4, Curve C), demonstrating that reasonable image quality can be achieved. The coincidence counting

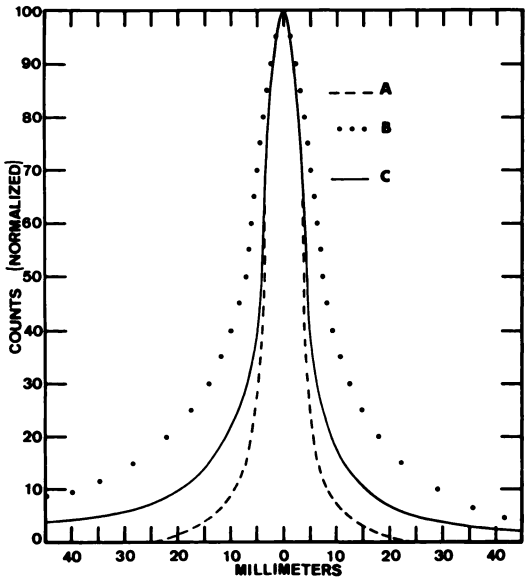

FIG. 4. Line-spread functions in presence of scatter material: A, photopeak–photopeak, 260 cps; B, Compton–Compton, 480 cps; and C, all four possible combinations, 1,400 cps.

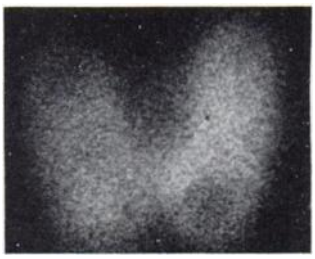

FIG. 5. Image of thyroid phantom submerged in water as scatter material (150,000 counts, 20 sec).

rate in Fig. 5 was 7,500 cps at a singles rate of 110,000 cps and counting rates twice as high have been obtained at some loss in image quality due to random coincidence counts.

MAXIMUM COUNTING RATE

By using the pulse-handling scheme shown in Fig. 3 where even the integration of the light output occurs only for the relatively few pulses (less than 10%) which are found in coincidence, deadtime can be kept to a minimum. Indeed, singles counting rates (discriminator output pulses) as high as 400,000 cps have been obtained without significant distortion of position pulses. The major limitation in the maximum useful counting rate is now not the maximum rate at which each detector can be operated but the maximum random coincidence rate which is acceptable. The fast coincidence circuit accepts two pulses as coincident if they occur within some small time interval, in these experiments 20 nsec. As the rate in each detector increases, the probability of two noncoincident events accidentally falling within this time interval increases. The random coincidence rate R_R is given by:

$$R_R = 2\tau R_1 R_2$$

where R_1 and R_2 are the discriminator output rates from the two detectors and the quantity 2τ is the resolving time of the coincidence circuit. While R_R is only a small fraction of R_1 or R_2, the true coincidence rate, R_T, is also only a small fraction of R_1 or R_2. In order to achieve a high true coincidence rate without excessive random coincidences, the resulting time must be kept to a minimum and R_T/R_1 and R_T/R_2 must be maximized, i.e., as many of detected events as possible must be made useful. It is in this last respect that a significant improvement has been achieved. The graded absorber eliminates scattered and therefore useless gamma rays from entering the crystal and by using dual windows a larger fraction of the events which are detected are being used to form the image. A significant fraction of primary gamma rays, however, either scatters in the object or does not interact in the scintillation crystal. Whereas previously in a similar experimental arrangement (*3*), R_T/R_1 was found to be 0.01, we measured $R_T/R_1 = 0.07$, i.e., 7% of all detected counts are used to form the image. In actual patient studies this quantity is likely to fall to 2% due to counts from outside the geometric coincidence aperture entering one of the detectors. Assuming $R_1 = R_2 = 200{,}000$ cps and a resolving time (2τ) of 20 nsec, a random coincidence rate of 800 cps is obtained while the true coincidence rate (2% of R_1) is 4,000 cps. This is sufficient for static imaging and slow function studies but precludes the use of the present system in fast dynamic studies.

The factors limiting the resolving time of our system are not well understood yet and are presently being studied. We have found that improving the preamplifier risetime improved the resolving time. In addition, transit time variations in the photomultipliers seem to be a major factor, suggesting the possibility that the transit time from each photomultiplier may have to be adjusted to further improve resolving time. As we understand the factors limiting resolving time better, we can expect further improvements; resolving times well below 5 nsec are achieved in optimized state-of-the-art systems (*8*).

GEOMETRY

In the results reported here, the object was placed in the plane of best focus midway between both detectors. An analog multiplane display is currently being built which will show several planes in focus simultaneously. The depth of focus is a function of

the separation between detectors. In order to be able to shield effectively against radiation from outside the geometric coincidence aperture in clinical trials, we intend to use a separation of approximately 30 in. and a circular shield of either 5 in. or 9 in. on each detector, which results in a depth of focus of approximately 1 in. The reconstruction of images formed using rays differing widely in angle poses both a challenge and an opportunity; computer reconstruction of the three-dimensional object distribution in a system using a similar geometry is currently being attempted by others (*9*).

CONCLUSION

It has been shown that Compton events in the scintillation crystal followed by escape of the secondary gamma ray can be used to form an image in a positron camera if gamma rays scattered in the object are largely eliminated by absorbers. In the particular positron camera investigated here (two opposing ½-in.-thick NaI crystals) the coincidence counting rate could be increased fivefold.

This technique should be applicable to a large class of devices. While it has not been shown here, it appears that Compton events in the crystal can also be used in systems such as normal Anger scintillation cameras to form an image from single (noncoincident) events. The use of this technique is, however, restricted to higher energies such as 510 keV since at much lower energies the scattered radiation from the object is not sufficiently different from the primary gamma ray energy to be effectively rejected through the use of absorbers. Indeed, it is only at the higher energies that this technique becomes desirable since at low energies Compton events followed by the escape of the secondary gamma ray occurs relatively infrequently.

REFERENCES

1. BROWNELL GL, BURNHAM CA: Recent developments in positron scintigraphy. In *Instrumentation in Nuclear Medicine*, vol 2, Hine GJ, Sorenson JA, eds, New York, Academic Press, 1973, pp 135–159

2. ANGER HO: Radioisotope cameras. In *Instrumentation in Nuclear Medicine*, vol 1, Hine GJ, ed, New York, Academic Press, 1967, pp 485–550

3. KENNY PJ: Spatial resolution and countrate capacity of a positron camera: some experimental and theoretical considerations. *Int J Appl Radiat Isot* 22: 21–28, 1971

4. MUEHLLEHNER G, JASZCZAK RJ, BECK RN: The reduction of coincidence loss in radionuclide imaging cameras through the use of composite filters. *Phys Med Biol* 19: 504–510, 1974

5. ANGER HO, DAVIS DH: Gamma-ray detection efficiency and image resolution in sodium iodide. *Rev Sci Instrum* 35: 693–697, 1964

6. EICHLING JO, TER-POGOSSIAN MM, RHOTEN AL: Analysis of the scattered radiation encountered in lower energy diagnostic scanning. In *Fundamental Problems in Scanning*, Gottschalk A, Beck RN, eds, Springfield, Ill, Thomas, 1968, p 238

7. BECK RN, SCHUH MW, COHEN TD, et al: Effects of scattered radiation on scintillation detector response. In *Medical Radioisotope Scintigraphy*, vol 1, Vienna, IAEA, 1969, p 595

8. VAN ZURK, LOPES FB, ROS J: Circuit de déclenchement, avec réjection du bruit, pour mesures temporelles à basse énergie avec compteurs NaI(Ti). *Nucl Instrum Meth* 120: 61–68, 1974

9. PEREZ-MENDEZ V: Personal communication, 1974